Cooperative light-induced molecular movements of highly ordered azobenzene self-assembled monolayers

Giuseppina Pace*, Violetta Ferri†, Christian Grave†, Mark Elbing‡§, Carsten von Hänisch‡, Michael Zharnikov¶, Marcel Mayor‡‖**, Maria Anita Rampi†**, and Paolo Samorì*,**††

*Unité Mixte de Recherche 7006, Institut de Science et d'Ingénierie Supramoléculaires/Centre National de la Recherche Scientifique, Université Louis Pasteur, 8 Allée Gaspard Monge, F-67083 Strasbourg, France; †Dipartimento di Chimica, Università di Ferrara, 44100 Ferrara, Italy; ‡Forschungszentrum Karlsruhe, Institute for Nanotechnology, P.O. Box 3640, D-76021 Karlsruhe, Germany; ¶Angewandte Physikalische Chemie, Universität Heidelberg, Im Neuenheimer Feld 253, D-69120 Heidelberg, Germany; ‖Department of Chemistry, University of Basel, St. Johannsring 19, CH-4056 Basel, Switzerland; and ††Istituto per la Sintesi Organica e la Fotoreattività, Consiglio Nazionale delle Ricerche, Via Gobetti 101, I-40129 Bologna, Italy

Edited by Jean-Marie P. Lehn, Université Louis Pasteur, Strasbourg, France, and approved April 25, 2007 (received for review February 2, 2007)

Photochromic systems can convert light energy into mechanical energy, thus they can be used as building blocks for the fabrication of prototypes of molecular devices that are based on the photomechanical effect. Hitherto a controlled photochromic switch on surfaces has been achieved either on isolated chromophores or within assemblies of randomly arranged molecules. Here we show by scanning tunneling microscopy imaging the photochemical switching of a new terminally thiolated azobiphenyl rigid rod molecule. Interestingly, the switching of entire molecular 2D crystalline domains is observed, which is ruled by the interactions between nearest neighbors. This observation of azobenzene-based systems displaying collective switching might be of interest for applications in high-density data storage.

scanning tunnel microscopy | molecular switches | photochromic system | data storage

Single molecules can be functional; i.e., they can be designed to store information and to perform preprogrammed actions, thereby to act as a machine (1–4). Nature exploits, to a great extent, light energy as energy inputs because it is environmentally friendly and everlasting. Among photochromic molecules (5–10), azobenzenes have been extensively studied for their unique photoisomerization. The transition from the thermodynamically more stable trans to the cis conformation can be induced by irradiation with UV light and reversed upon heating or irradiation with visible light. Such photochemical trans ↔ cis isomerization of azobenzene was first described by Krollpfeiffer *et al.* (11), and it has been thoroughly studied in the last decades (12, 13). Many applications profiting from the conformational rearrangement of the molecule, such as optical data storage devices (14, 15), switchable supramolecular cavities and sensors (16), or light-powered molecular machines delivering mechanical work (17, 18), have been proposed. The reversible switching of azobenzene derivatives has already been investigated at room temperature on the single-molecule level by scanning tunneling microscopy (STM) experiments in ultra-high vacuum studies on isolated molecules packed parallel to the basal plane of the substrate (19–21), in physisorbed monolayers at the solid-liquid interface (22, 23), on self-assembled monolayers (SAMs) chemisorbed on Au nanoparticles (24), and as coadsorbate in a chemisorbed alkyl thiolated SAM on solid flat substrates (25). However, conformationally flexible alkylthiols exposing azobenzene head-groups forming single component SAMs have been reported being either non or poorly responsive to light excitation. Moreover, similarly to the case of Langmuir–Blodgett films incorporating azobenzenes (26), the photoinduced isomerization has not been thoroughly characterized down to the nanoscale to provide unambiguous evidence for its occurrence, and no explanation has been given regarding the conformational reorganization within the SAM after the isomerization. To overcome this problem, photoisomerization was indeed accomplished in the past by "diluting" the function, i.e., by incorporating the azobenzene-containing molecule in a shorter alkanethiol SAM matrix (25). Unfortunately, in this latter case, neither a precise structural picture of the conformation of the azobenzene molecules in the hosting SAM before and after the switch nor a high level of understanding of the structural reorganization of the hosting domain upon interconversion of the guest molecules could be achieved. In addition, it was not possible to unambiguously ascribe the azobenzene isomerization to either a single or a few molecules adsorbed at defect sites. This is indeed because of the fact that the photoinduced interconversion of single molecules of both azobenzenes (25) and other photochromic systems, e.g., diarylethenes (27), chemisorbed in a hosting alkanethiol monolayer was observed only for molecules adsorbed at domain boundaries. In such locations, the molecules are weakly anchored to the substrate and loosely packed and therefore less stable and thus more subjected to fluctuations.

We designed a fully conjugated oligomer (**1**) (see chemical formula in Fig. 1) adapted to chemisorb on Au(111) surfaces into a single-component SAM, with a packing motif similar to that of arenethiols. This packing potentially enables, from the steric viewpoint, single molecules arranged in the densely packed and crystalline architecture to undergo isomerization. Moreover, **1** has been tailored to possess a high conformational rigidity, which differs from more conformationally flexible thiolated azobenzenes bearing aliphatic units. In fact, SAMs of arenethiols differ from those of alkanethiols for the rigid character of the molecular components. The π-conjugated backbone is responsible for T-shaped interactions among the π-states that give rise to the herringbone structure characterizing SAMs of arenethiols. In aromatic SAMs, the π–π intermolecular interactions are mostly responsible for the geometry of the 2D packing on the Au(111) surface, whereas in alkanethiol SAMs, such geometry is primar-

Author contributions: M.M., M.A.R., and P.S. designed research; G.P., V.F., C.G., and M.E. performed research; M.E. and M.M. contributed new reagents/analytic tools; G.P., V.F., C.v.H., and M.Z. analyzed data; and G.P., M.M., M.A.R., and P.S. wrote the paper.

The authors declare no conflict of interest.

This article is a PNAS Direct Submission.

Abbreviations: SAM, self-assembled monolayer; STM, scanning tunnel microscopy; UV/Vis, UV-visible.

§Present address: Department of Chemistry, Center for Polymers and Organic Solids, University of California, Santa Barbara, CA 93106.

**To whom correspondence may be addressed. E-mail: marcel.mayor@unibas.ch, rmp@unife.it, or samori@isis-ulp.org.

This article contains supporting information online at www.pnas.org/cgi/content/full/0703748104/DC1.

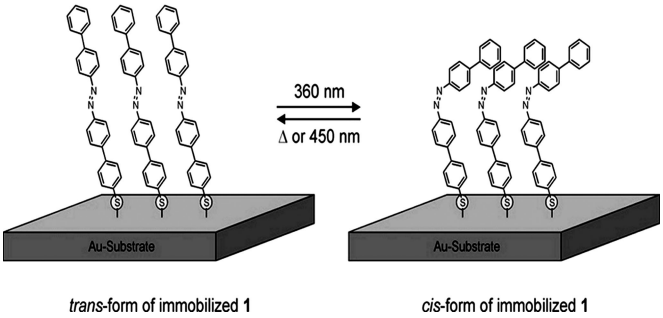

Fig. 1. Cartoon of the switching molecule on an Au surface. For the sake of example, a small domain of molecule 1 [4′-(biphenyl-4-ylazo)-biphenyl-4-thiol] immobilized on a Au surface has been sketched. Intermolecular interactions between adjacent molecules stabilize the packing of domains consisting exclusively of trans-isomers (*Left*), as well as the packing of domains consisting exclusively of cis-isomers (*Right*).

ily governed by the sulfur head group–substrate interaction (28). Finally, **1**, because of its similar structure to arenethiols, can be expected to posses an essentially planar conformation enabling a tight packing at the supramolecular level originated by π–π intermolecular interactions. We describe herein the nanoscale-resolved visualization of the trans ↔ cis switching occurring at surfaces by means of STM imaging. Such spatially resolved mapping makes it possible to gain insight into the isomerization mechanism and yield. The conclusions derived on the basis of the STM data are corroborated by UV-visible (UV/Vis) spectroscopy results.

Results and Discussion

Photochemical studies in chloroform solutions revealed that our molecule represents an optically addressable molecular switch that can undergo trans ↔ cis photoisomerization, as monitored by UV-Vis spectroscopy [see Fig. 2*B* and supporting information (SI) Figs. 5 and 6]. ^{1}H-NMR studies in solution upon light irradiation provided evidence for the formation of a photostationary state with a trans → cis conversion of 88%, and a back thermal isomerization characterized by a first-order reaction with a rate constant $k = 8.6{\cdot}10^{-4}$ sec^{-1} (SI Fig. 7) (29). Optical studies performed in transmission mode revealed spectral changes upon subsequent irradiations at $\lambda = 450$ nm and $\lambda = 360$ nm of SAMs chemisorbed both on transparent Pt and Au surfaces as displayed in Fig. 2*A* and SI Fig. 8, respectively. The spectra in Fig. 2*A* unequivocally show the reversible character of the switching process on solid substrates. The stability and reversibility of the signal detected during the lifetime of a device is of paramount importance when evaluating the use of an organic compound for molecular device applications. The photoconversion of the photostationary state within the SAM was calculated to span between 94% and 100% (see *Methods*). The back thermal reaction on the surface is dominated by a first-order kinetic with a rate constant $k = 1.33{\cdot}10^{-4}$ sec^{-1} (SI Fig. 9). These values indicate clearly that the cis → trans thermal reaction is slower when **1** is organized in SAMs if compared with **1** dissolved in a chloroform solution.

STM studies of the chemisorbed monolayer made it possible to investigate the structural and light-induced dynamical properties of **1** on Au(111) with a molecular resolution. A SAM of **1** was prepared by incubating the substrate under dark condition overnight and studied at the solid–air interface. The STM image in Fig. 3*A* shows a monocrystalline domain: each bright spot represents a single molecule adopting the trans conformation. The densely packed and highly ordered 2D architecture exhibits a herringbone structure with a rectangular unit cell ($a = 0.65 \pm 0.05$ nm, $b = 0.89 \pm 0.05$ nm, and $\alpha = 84° \pm 5$) containing two molecules. Such packing is in very good agreement with that of arenethiol SAMs (30) and azobenzene alkylthiolated molecules chemisorbed on Au(111) (31, 32). In such a crystalline motif, the molecules pack more perpendicularly to the Au(111) surface if compared with alkanethiol SAMs.

The same film was then irradiated for 15 min at 365 nm to activate the trans → cis isomerization. Fig. 4*A* displays an STM image recorded 90 min after the irradiation. In the image, a single cis molecule is marked by the oval. The upper part of the image exhibits molecules mostly isomerized in the cis conformation, whereas the lower part is mainly dominated by the trans conformer. In Fig. 4, the profiles I and II are traced across the molecules adopting a cis and a trans conformation, respectively. Both profiles I and II exhibit a constant distance between binding sites, which amounts to 8.8 Å. However, in profile I, each molecule displays two peaks separated by a distance of 2.6 Å, which represents a fingerprint of the cis isomer. This value is not directly related to the distances calculated according to the atomic (geometrical) model. In fact, the tunneling is governed by the overlap of the tip's density of state with well defined molecular orbitals containing the contribution of the molecule–substrate interaction. Therefore, the measured distance between the two spots of a cis molecule should be explained in terms of the shape of the molecular orbitals contributing to the tunneling and not according to the distances between the atoms or groups. The cis molecule appears in the STM current images as formed by two spots. The high electron density at the Au–S bond has been shown to originate a high contrast in STM images, allowing the easy identification of the Au-thiols binding sites (33). Therefore, we attribute the brighter spot to the straight biphenyl-

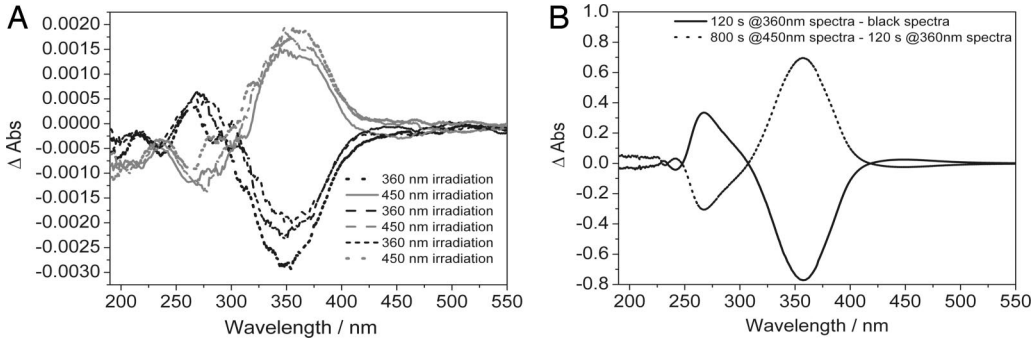

Fig. 2. Absorption spectra of the reversible switching of **1** in a SAM on Pt and in a solution. (*A*) UV/Vis spectral changes upon photoisomerization of **1** arranged in SAMs on Pt surfaces. The SAM of **1** has been switched back and forth between the trans and the cis conformer by irradiating the sample with UV light at 450 and 360 nm, respectively. After each switching process, absorption spectrum were recorded. The curves shown have been obtained by subtracting two subsequent absorption spectra. (*B*) UV/Vis spectral changes upon photoisomerization of **1** in chloroform solution.

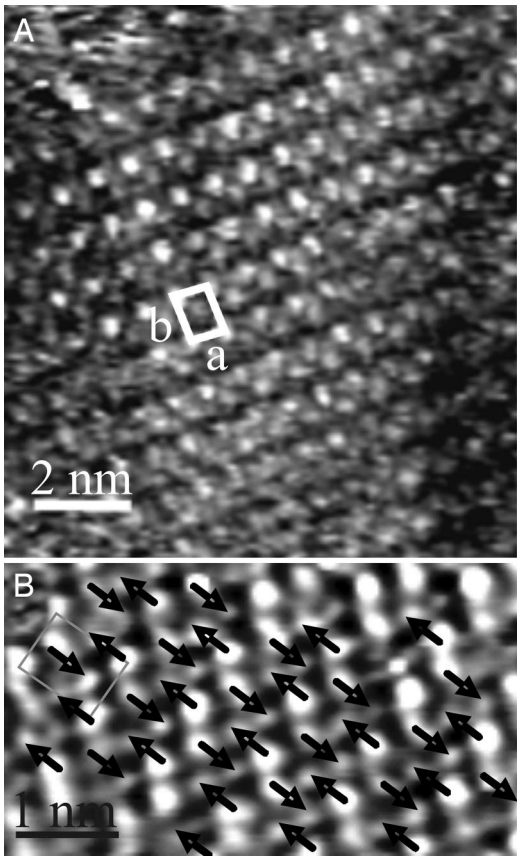

Fig. 3. STM images of the trans and cis domain. (*A*) Constant-current STM image of *trans*-AZO SAM on Au(111) showing a rectangular unit cell containing two molecules ($a = 0.65 \pm 0.05$ nm, $b = 0.89 \pm 0.05$ nm, and $\alpha = 84° \pm 5$). Average tunneling current (I_T) = 55 pA; bias voltage (V_T) = 150mV. (*B*) STM image showing a cis domain of a sample prepared by incubating overnight the Au(111) substrate in solution of **1** under light irradiation at 365 nm. After removal from the incubating solution, the sample was further irradiated for 90 min before imaging. The picture has been recorded ≈30 min after irradiation. $I_T = 13.22$ pA; $V_T = 280$ mV. The arrows indicate the direction of the bending during the switch of each molecule in the domain.

thiolated side of the aromatic chain (34). Consequently, the second spot corresponds to the terminal biphenyl side group of the aromatic chain that is relocated upon isomerization. The isomerization to the cis conformation brings the upper biphenyl side of the chain closer to the gold surface. In such a position, the biphenyl moiety electronically interacts with the substrate; a tunneling-through-space process allows the monitoring of these molecular segments by STM.

The unit cell parameters found for the cis domains, which amount to $a = 0.62 \pm 0.05$ nm, $b = 0.81 \pm 0.05$ nm, and $\alpha = 88° \pm 5$, are identical to those of the trans domains, within the experimental error bars, strongly supporting an isomerization mechanism without rearrangements at the Au-sulfur binding sites. Thus, only a conformational transition of the aromatic chain takes place, which is presumably accompanied by a change in the molecular tilt to compensate for the difference in the molecular volume between the trans and cis conformers. The same lattice parameters of the cis unit cell have been found chemisorbing the cis conformer on the Au substrate. This sample was prepared by incubating the gold surface overnight in a solution of **1** under light irradiation (at 365 nm) and further irradiating for 90 min after removal from the solution (Fig. 3*B*). This experimental evidence is relevant, because it suggests that both cis and trans conformers can chemisorb into thermodynamically stable and highly ordered crystalline films. Like the trans domains, the cis domains adopt a herringbone structure, proving that the π–π intermolecular interactions are also responsible for the stability of the cis domains. In previous studies, *cis*-azobenzene derivatives have been physisorbed only flat on Au(111) by a prior irradiation of the azobenzene solutions, but it was not possible to form ordered cis domains starting from the trans conformers adsorbed on the gold (35). Significantly, in Fig. 3*B*, it is possible to identify the bending direction of the switching molecules, as indicated by the arrows. Inside a cis-unit cell, the two molecules isomerize, bending the upper biphenyl side in opposite directions. The unidirectionality of the switch occurring on adjacent molecules along the direction of the unit cell main axis, together with the opposite orientation of bending in neighboring rows, is caused by the minimization of steric hindrance. Because the trans binding sites seem to not be disturbed by the switching process, we deduce that the intermolecular interactions between the cis molecules stabilize the herringbone structure of the new cis domain, which is further corroborated by the slow thermal back-isomerization detected for the SAMs by UV-Vis absorption measurements.

We showed that the isomerization is extended over many adjacent molecules arranged into a few tens of nanometers-wide crystalline domain. The observation of such a long-range switching, means that the yield of conversion on a domain of the trans conformer is nearly complete, i.e., it is higher than the isomerization yield in solution, as also documented by optical spectroscopy. This long-range order can be ascribed to a cooperative process that determines the long-range conversion. Upon the initial isomerization of a few molecules, the intermolecular interactions between the switched molecules and the surrounding trans isomers are most likely weakened, promoting the isomerization of other adjacent molecules along the unit cell main axis direction, a mechanistic picture that is further supported by the unidirectional character of the bending. The possibility to stabilize the cis conformer through the intermolecular interactions among adjacent molecules in a cis domain is responsible for the considerably increased yield of the isomerization on the solid substrate with respect to the solution yield. This consideration is corroborated by the value of the kinetic constant calculated for the thermal back cis → trans reaction on metal surface, which is more than seven times lower than in solution. The rigidity of the aromatic backbone is responsible for the cooperative switch and the π–π interchain interactions are fundamental for the long lifetime of the cis isomer at surface. In fact, upon switching of one molecule, the number of accessible conformations (i.e., relaxation states) of adjacent molecules, leading to a decrease of the free energy of the domain, is limited by the rigidity of the backbone. Such reduced number of conformations that can be adopted to stabilize the cis domains favors the occurrence of a cooperative and unidirectional switch. The absence of this cooperative effect might be the reason why the so-far reported systems consisting of bidimensional crystals of alkylthiols exposing azobenzene head groups (31, 32) did not display comparable switching properties; in fact, both requirements, i.e., rigidity and π–π interchain interactions, were not fulfilled.

Conclusions

In summary, we have shown that a properly designed azobenzene molecule can undergo cis-trans photoisomerization in large domains at surfaces. This switch, which occurs in densely packed single-component SAMs without perturbing the molecular lattice, is complete over hundreds of molecules, and it exhibits a cooperative character. Such a cooperative process is previously unexplored and widely applicable for switchable single-component SAMs consisting of intrinsically rigid and tightly packed molecules, given that the mechano-chemical switch is not

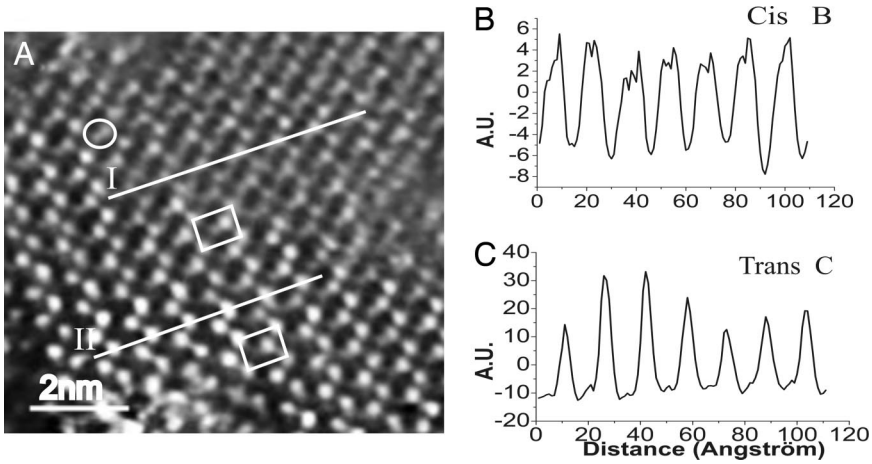

Fig. 4. Cooperative switching occurring over a single molecular domain. (*A*) STM image of SAM of **1** formed on stripped Au(111) incubated in the dark for one night in $5{\cdot}10^{-4}$ M solution in toluene. In the image, a single cis molecule is marked by the oval. The sample was irradiated for 15 min before measurements. The image was recorded 90 min after the irradiation. This time frame is very small if compared with the 2 weeks needed to achieve a complete restoration of the trans isomer of alkyl-thiolated *cis*-azobenzenes under dark (42). The lower unit cell contains the trans isomers; the upper unit cell contains cis molecules. The profiles are traced along the direction of the unit cell main axis, i.e., the direction of the switch (see Fig. 2*B*) $I_T = 49.00$ pA; $V_T = 145$ mV. (*B* and *C*) Line profiles showing profile I the cis conformer (*B*) and profile II the *trans* conformer (*C*). The two spots were observed to be located in identical positions also upon changing systematically the scan angle and scan rate, as well as on different samples and employing different tips, therefore ruling out any imaging artifact. Moreover, the switch was visualized by STM by using various tunneling parameters and therefore diverse tunneling gap impedances. Thus, although we cannot fully neglect a mechanical or electrical contribution of the tip to the switch, we do believe it does not hold a prime role. Although the isomerization occurs over some hundreds of adjacent molecules, it does not take place over the whole sample surface.

sterically hindered. Therefore, it opens new avenues for the design of molecules capable of switching in a controlled fashion over a monolayer. The high yield of the cis-trans isomerization on metal substrate opens intriguing perspectives for high-density data storage devices (36) on the basis of photochromic compounds. Our long-range photoisomerization taking place on the surface was not observed in previous STM studies performed at the solid–liquid interface, because the dynamic exchange between the supernatant solution and the adsorbate did not allow the unambiguous determination of whether the isomerization was occurring on the surface or in the solution through a subsequent desorption and readsorption process (22, 23). This system is ideal to implement in crossbar memories and for the achievement of light-driven logic operations (37). A monolayer of photoisomerizable molecules embedded in a molecular switch tunnel junction can be used as a data storage element (bit) (36). Current activity is addressed toward the assessment of crucial parameters as switching speeds and potential degradation of molecular components. Moreover, the fully conjugated molecular structure of our building blocks renders our highly ordered SAM a unique workbench for molecular devices, in particular for nanomechanical and nanoelectronic applications.

Methods

Synthesis and Characterization. The target structure, i.e., 4′-(biphenyl-4-ylazo)-biphenyl-4-thiol (**1**), has been assembled in a seven-step synthesis displayed in Scheme 1. The key steps were the formation of the azo linkage in a Mills reaction (38) between 4-nitrosobiphenyl and 4-amino-4′-methylsulfoxybiphenyl to form a suitable precursor, which was converted to **1** by a Pummerer rearrangement followed by *in situ* hydrolysis (39). The newly synthesized compounds have been characterized by ^{1}H-

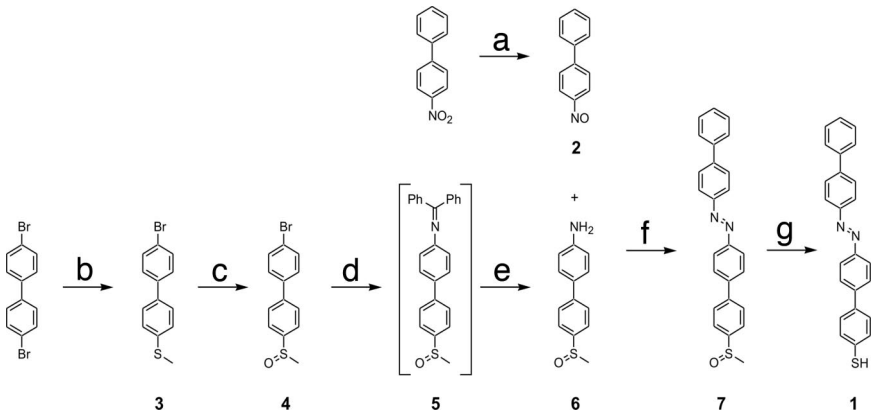

Scheme 1. Synthesis of the azo-functionalized rod 1 comprising a terminal sulfur group. (Reaction a) Step 1: NH_4Cl, Zn, $MeOCH_2CH_2OH$, and H_2O at 35°C. Step 2: $FeCl_3$, $MeOCH_2CH_2OH$, H_2O, and EtOH at −5°C, 63%. (Reaction b) NaSMe and DMI at 150°C, 60%. (Reaction c) mCPBA and CH_2Cl_2 at 0°C, 89%. (Reaction d) $(Ph)_2C = NH$, $[Pd_2(dba)_3]{\cdot}CHCl_3$, KOtBu, BINAP, and $CH_3C_6H_5$ at 80°C, 77%. (Reaction e) $NH_2OH{\cdot}HCl$, NaOAc, and MeOH at room temperature, 95%. (Reaction f) AcOH and CH_2Cl_2 at 65°C, 83%. (Reaction g) Step 1: $(CF_3CO)_2O$ and $CH_3C_6H_5$ at 40°C. Step 2: Et_3N, $CH_3C_6H_5$ and EtOH, at room temperature, 27%. Detailed information on the synthesis and characterization are given in the *SI Text*.

NMR and ^{13}C-NMR spectroscopy, mass spectrometry, and elemental analysis. However, the poor solubility, together with the limited availability of **1**, did not allow a ^{13}C-NMR spectrum to be recorded. In view of the x-ray structure of the precursor **7** (see *SI Text* and SI Fig 10) already comprising the biphenyl-azo substructure, we assume that both biphenyl subunits are essentially planar, and due to the planar character of the $N = N$ group, all moieties reside in the same plane. The planar structure leads to strong π–π stacking interactions between neighboring molecules in the solid state, resulting in very limited solubility of **1** in organic solvents.

Monolayers Preparation. For UV measurements, Pt and Au films with a nominal thickness of 10 nm have been prepared on quartz by E-Beam deposition and vacuum sublimation, respectively. STM measurements have been carried out on gold evaporated on mica substrates (100-nm thick). The SAMs were prepared by immersion of freshly prepared metallic substrates into a 0.1 mM solution of **1** in degassed chloroform at room temperature for 24–48 h. After immersion, the samples were carefully rinsed with pure chloroform and blown dry with argon.

UV/Vis Spectroscopy and Photoirradiation. UV/Vis spectra have been recorded with a Kontron (Zurich, Switzerland) Uvikon 931 spectrophotometer. The irradiation of the SAMs of **1** has been performed *in situ* inside the spectrophotometer cavity. The irradiation cycles have been executed with a Spectral Luminator (LOT-Oriel, Stamford, CT). The exposure time of the irradiation has been indicated in the figures. Measurements on SAM on Pt and Au substrates were carried out under nitrogen to avoid the substrate oxidation. The bandwidth of the light source in the UV/Vis region was 5 nm. The photoisomerization of the SAM has been measured as spectral differences to reduce the interference of the metal absorption band. Pt metal surface has been used as a solid substrate to record the spectral differences related to the trans-cis isomerization without the contribution of the changes in surface plasmon bands of the metal.

Kinetical Studies of the Trans-Cis Isomerization in Solution and on the Surfaces. The yield of the photoconversion in solution of **1** from the trans to the cis form has been calculated from the ratio of the ^{1}H-NMR signals of the two isomers in the initial and in the photostationary state. The spectrum of the cis form has been calculated combining the data of the percent of the photoconversion from trans to cis form obtained form the ^{1}H-NMR spectra and the related UV-Vis spectra. The spectra of the measured trans and the calculated cis form in solution are reported in *SI Text* and SI Figs. 7 and 9.

We have calculated the trans → cis photoconversion yield at the photostationary state of **1** in the SAMs on Pt and on Au by assuming that the values of the extinction coefficients of the cis and trans forms do not change upon organization on SAMs, because they are only slightly dependent on their environment (40, 41). Under this approximation, the trans → cis photoconversion yield has been obtained by deconvolution of the absorption spectra of the photostationary state.

The thermal cis → trans back isomerization of **1**, both in solution and in SAMs, has been followed by recording the increase of UV/Vis spectra at $\lambda = 360$ nm. From these data, the lifetimes and the constant rates were calculated. The kinetic constants reported in the main text for the back thermal reaction in solution, on Pt and on Au surfaces, are calculated according to a first-order kinetic equation.

STM. STM images were obtained in constant-current mode with a commercial apparatus (Multimode Nanoscope IV; Veeco, Woodbury, NY) in air and at room temperature. The STM tips were cut from a Pt/Ir wire (0.25 mm). Unit cells were averaged over several images, making use of SPIP software [Scanning Probe Image Processor (SPIP), version 2.0; Image Metrology, Lyngby, Denmark].

Substrate and Monolayer Preparation. Au(111) terraces were obtained by flame annealing of gold evaporated on a mica substrate. The *trans*-SAMs were formed after overnight incubation in the dark of the Au(111) in a $5{\cdot}10^{-4}$ M solution of **1** in toluene or $CHCl_3$.

Complete details of methods used are given in *SI Text*.

This work was supported by the European Union through Marie Curie Early Stage Research Training SUPER Grant MEST-CT-2004-008128, The Light-Induced Molecular Movements Grant IST-2001-35503, the Marie Curie Reasearch Training Network PRAIRIES Grant MRTN-CT-2006-035810 and THREADMILL Grant MRTN-CT-2006-036040, the European Research Area Chemistry Project SurConFold, the European Science Foundation SONS2 SUPRAMATES Project, the Regione Emilia-Romagna PRIITT Nanofaber Net-Lab, Deutsche Forschungsgemeinschaft Grant ZH 63/9-2, and the Swiss National Center of Competence in Research Nanoscience of the Swiss National Science Foundation.

1. Balzani V, Credi A, Raymo FM, Stoddart JF (2000) *Angew Chem Int Ed* 39:3349–3391.
2. Raymo FM (2002) *Adv Mater* 14:401–414.
3. Browne WR, Feringa BL (2006) *Nature Nanotechnology* 1:25–35.
4. Kay ER, Leigh DA, Zerbetto F (2007) *Angew Chem Int Edit* 46:72–191.
5. Koumura N, Zijlstra RWJ, van Delden RA, Harada N, Feringa BL (1999) *Nature* 401:152–155.
6. Brouwer AM, Frochot C, Gatti FG, Leigh DA, Mottier L, Paolucci F, Roffia S, Wurpel GWH (2001) *Science* 291:2124–2128.
7. Hernandez JV, Kay ER, Leigh DA (2004) *Science* 306:1532–1537.
8. Mobian P, Kern JM, Sauvage JP (2004) *Angew Chem Int Edit* 43:2392–2395.
9. Balzani V, Clemente-Leon M, Credi A, Ferrer B, Venturi M, Flood AH, Stoddart JF (2006) *Proc Natl Acad Sci USA* 103:1178–1183.
10. Irie M (2000) *Chem Rev* 100:1685–1716.
11. Krollpfeiffer F, Muhlhausen C, Wolf G (1934) *Annalen* 508:39–51.
12. Griffiths J (1972) *Chem Soc Rev* 1:481–493.
13. Tamai N, Miyasaka H (2000) *Chem Rev* 100:1875–1890.
14. Liu ZF, Hashimoto K, Fujishima A (1990) *Nature* 347:658–660.
15. Ikeda T, Tsutsumi O (1995) *Science* 268:1873–1875.
16. Shinkai S (1987) *Pure Appl Chem* 59:425–430.
17. Yu YL, Nakano M, Ikeda T (2003) *Nature* 425:145.
18. Hugel T, Holland NB, Cattani A, Moroder L, Seitz M, Gaub HE (2002) *Science* 296:1103–1106.
19. Henzl J, Mehlhorn M, Gawronski H, Rieder KH, Morgenstern K (2006) *Angew Chem Int Ed* 45:603–606.
20. Choi BY, Kahng SJ, Kim S, Kim H, Kim HW, Song YJ, Ihm J, Kuk Y *Phys Rev Lett* (2006) 96:156106.
21. Alemani M, Peters MV, Hecht S, Rieder KH, Moresco F, Grill L (2006) *J Am Chem Soc* 128:14446–14447.
22. De Feyter S, Gesquiere A, Abdel-Mottaleb MM, Grim PCM, De Schryver FC, Meiners C, Sieffert M, Valiyaveettil S, Mullen K (2000) *Acc Chem Res* 33:520–531.
23. Feng CL, Zhang YJ, Jin J, Song YL, Xie LY, Qu GR, Jiang L, Zhu DB (2002) *Surf Sci* 513:111–118.
24. Zhang J, Whitesell JK, Fox MA (2001) *Chem Mater* 13:2323–2331.
25. Yasuda S, Nakamura T, Matsumoto M, Shigekawa H (2003) *J Am Chem Soc* 125:16430–16433.
26. Matsumoto M, Miyazaki D, Tanaka M, Azumi R, Manda E, Kondo Y, Yoshino N, Tachibana H (1998) *J Am Chem Soc* 120:1479–1484.
27. Katsonis N, Kudernac T, Walko M, van der Moten SJ, van Wees BJ, Feringa BL (2006) *Adv Mater* 18:1397–1400.
28. Cyganik P, Buck M, Strunskus T, Shaporenko A, Wilton-Ely JD, Zharnikov M, Wöll C (2006) *J Am Chem Soc* 128:13868–13878.
29. Tamada K, Akiyama H, Wei TX (2002) *Langmuir* 18:5239–5246.
30. Azzam W, Fuxen C, Birkner A, Rong HT, Buck M, Wöll C (2003) *Langmuir* 19:4958–4968.
31. Mannsfeld SCB, Canzler TW, Fritz T, Proehl H, Leo K, Stumpf S, Goretzki G, Gloe K (2002) *J Phys Chem B* 106:2255–2260.

32. Evans SD, Johnson SR, Ringsdorf H, Williams LM, Wolf H (1998) *Langmuir* 14:6436–6440.
33. Fitts WP, White JM, Poirier GE (2002) *Langmuir* 18:1561–1566.
34. Poirier GE (1997) *Langmuir* 13:2019–2026.
35. Xu LP, Wan LJ (2006) *J Phys Chem B* 110:3185–3188.
36. Green JE, Choi JW, Boukai A, Bunimovich Y, Johnston-Halperin E, DeIonno E, Luo Y, Sheriff BA, Xu K, Shin YS, *et al.* (2007) *Nature* 445:414–417.
37. Heath JR, Ratner MA (2003) *Phys Today* 56:43–49.
38. Feuer H (1969) *The Chemistry of the Nitro and Nitroso Groups, Pt 1: The Chemistry of Functional Groups*, (Interscience, New York).
39. Young RN, Gauthier JY, Coombs W (1984) *Tetrahedron Lett* 25:1753–1756.
40. Lakowicz JR (2001) *Anal Biochem* 298:1–24.
41. Pedrosa JM, Romero MTM, Camacho L, Möbius D (2002) *J Phys Chem B* 106:2583–2591.
42. Wang ZX, Nygard AM, Cook MJ, Russell DA (2004) *Langmuir* 20:5850–5857.